Single IMU Displacement and Orientation Estimation of Human Center of Mass: A Magnetometer-Free Approach

note finali coverpage

(Article begins on next page)

04 July 2024

Single IMU Displacement and Orientation Estimation of Human Center of Mass: A Magnetometer-Free Approach

Stefano Cardarelli, *Student Member, IEEE,* Alessandro Mengarelli, *Member, IEEE,* Andrea Tigrini,
Annachiara Strazza, *Student Member, IEEE,* Francesco Di Nardo, *Member, IEEE,*
Sandro Fioretti, *Member, IEEE,* and Federica Verdini

Abstract—In this paper, a self-contained procedure to estimate the vertical, medial-lateral, and anterior-posterior displacement of a single sacrum-worn inertial measurement unit (IMU) is presented, which can be related to the human body center of mass (CoM) displacement during treadmill walking through an adaptation of the sacral marker method. Further, a magnetometer-free custom sensor-fusion algorithm for orientation estimation is proposed alongside a practical alignment procedure to refer relative IMU orientation estimation to a ground-fixed reference frame. Twelve healthy subjects performed two trials of treadmill walking at 3, 4 and 5 km/h for 150 s, with a sacrum-worn IMU. Orientation and displacement estimations were then compared with those obtained from an optoelectronic measurement system. Roll, pitch and yaw angles showed root mean square errors (RMSE) lower than 2 deg for walking trials at 3, 4 and 5 km/h, with Pearson's correlation coefficient higher than 0.90 for each angle. Displacement accuracy was evaluated in terms of peak-to-trough distances and RMSE. Mean errors resulted lower than 1 mm for each axis of interest and for each gait speed, with RMSE not higher than 2.5 mm. The proposed off-line algorithm can be used in low-budget and infrastructure-free environments, to achieve reliable CoM displacement estimation during cyclic activities such as treadmill walking.

Index Terms—strapdown IMU, human body center of mass, treadmill walking, Unscented Kalman filter, 3-D displacement estimation, attitude estimation.

I. INTRODUCTION

IN the field of gait analysis, the 3-D motion of a subject's center of mass (CoM) is a valuable source of information, being a strong indicator of the overall biomechanical performance of walking [1]–[4]. Furthermore, CoM displacement has been associated to the evaluation of the risk of fall and pathological conditions in both adults and children [4]–[7]. The estimation of CoM displacement, therefore, represents a central issue in the movement analysis field and throughout the years a number of different techniques have been proposed in order to obtain an accurate spatial tracking of human CoM. According to the literature, the majority of studies relies on three main estimation methods [8], [9]. The first one is the segmental analysis and is based on the weighted sum of the CoM of single, body segments [8], [10], requiring an *a*

All authors are with the Department of Information Engineering, Università Politecnica delle Marche, Ancona, Italy (s.cardarelli@pm.univpm.it, a.mengarelli@pm.univpm.it, a.tigrini@pm.univpm.it, a.strazza@pm.univpm.it, f.dinardo@staff.univpm.it, s.fioretti@staff.univpm.it, f.verdini@staff.univpm.it)

priori knowledge of their mass distribution and an optoelectronic (OPT) system for kinematic measurements. The second method, based on force platforms measures, involves the application of inverse kinematic to estimate the CoM position from the double integration of ground reaction forces [1], [8], [9]. The third method relies on the assumption that a single marker placed over the sacrum can represent the CoM [11], [12] and due to its relatively easy marker setup, it is one of the most frequently used procedures for CoM estimation during dynamic tasks, and in particular during walking [9], [10]. On the other hand, despite these aspects, the sacral marker method remains limited in its applicability to OPT system instrumented environments, making this method barely usable in different experimental scenarios.

A possible way to overcome this limitation is the replacement of the sacral marker with a single inertial measurement unit (IMU) [10], [11], [13]. In this regard, the vertical (VT), medial-lateral (ML) and anterior-posterior (AP) displacement of the CoM can be hence ideally estimated simply through the double integration of the linear acceleration component measured by the IMU itself. Incidentally, in addition to the CoM displacement, the use of an IMU allows also to obtain the orientation of the body segment where the IMU is placed, i.e. the pelvis [14], [15]. The use of such method adaptation would imply a significant drop of costs and the enhancement of the measurement setup portability, making it particularly suitable for home-monitoring applications and in rehabilitation scenarios.

However, a crucial matter needs to be taken into consideration: the choice of the orientation estimation algorithm and a proper calibration procedure are both fundamental to refer IMU measurements (orientation and displacement) to an arbitrarily chosen ground-fixed reference frame (RF). An accurate orientation estimation is hence necessary to isolate the linear acceleration which is then used to estimate the IMU displacement, due to the fact that the gravitational acceleration is included in the readings of the accelerometer. Therefore, it is clear that the accuracy of the displacement estimation is strictly dependent on the accuracy of the orientation estimation.

In the gait analysis field, the instrumented treadmill appears to have widespread employment, providing a series of advantages over walking on the ground, allowing to perform a series of repetition of a cyclic function such as gait in a

controlled environment, at a repeatable and stable velocity, with a high number of consecutive steps. Further, a treadmill-based training has a key role as neuromotor therapeutic tool in promoting residual walking ability, being also particularly useful for the evaluation of pathological subjects in research and clinical contexts [4], [16], [17]. However, in motion analysis laboratories, magnetic disturbances are a common phenomenon that causes distortions in attitude estimation of an IMU [18]. In our particular scenario, such disturbances are generated by the treadmill electric motor and metallic structure, which affect the IMU magnetometer signal, leading to a bad computation of the sensor's orientation. For all these reasons, a magnetometer-free strapdown approach is proposed, in order to estimate the device relative orientation through an *Unscented* Kalman filter (UKF)-based sensor-fusion algorithm which relies only on accelerometer and gyroscope data. A calibration procedure is also proposed in order to refer the magnetometer-free orientation estimation to a ground-fixed navigation RF. This aspect was required also for validating the results with respect to an OPT system.

While the orientation estimation problem is commonly addressed through information filters, as Kalman-based or complementary, the inertial displacement estimation requires the use of the double integration of acceleration, where the drifting phenomenon can represent a crucial drawback, if not adequately treated. However, the unreliability of the simple, straightforward double integration of the signal coming from the accelerometer is well-acknowledged in the field of inertial sensing and dead-reckoning [19]. Thus, the double integration requires to be put into a theoretical (model) or experimental (zero-velocity updates) frame in order to temporally limit the drifting behavior. For this reason, in the field of human motion analysis, one of the most used approaches, also known as indirect estimation method, requires a geometrical model of human lower-limb [20], [21], being subject-dependent due to the need of anthropometric parameters. On the other hand, the methods based on zero-velocity update require the inertial sensor to be mounted on the foot in order to obtain the quasi-stationary periods needed for the integration and drift reset [22]. However, the latter method is mainly used for pedestrian dead-reckoning and cannot be directly employed for CoM displacement estimation, unless a biomechanical model and a multi-IMU approach are adopted [11].

The goal of the proposed work is hence to present a reliable procedure to estimate the 3-D human body CoM displacement, during treadmill walking by using a single inertial sensor, without the need for any biomechanical gait model and relying on the cyclic pattern of walking mechanics. To this aim, the sacral marker method was adopted, where the CoM trajectory is represented by the sacrum bone movement and the marker was replaced by a sacrum-worn IMU [10], [11], [13].

The choice of adopting the *Unscented* variant of the Kalman filter, over the well-established *Extended* version (EKF) [23], [24], was driven by the necessity to achieve high accuracies in spite of a missing sensor (magnetometer), following the intuition that the better performances of the UKF over the EKF [25], [26] would compensate the lack of magnetometer measurements. The core logic behind the UKF is that "*it is easier to approximate a probability distribution [than it is to] approximate an arbitrary nonlinear function or transformation*", and, as stated by Wan and Van Der Merwe, this can be achieved with a "*comparable level of complexity*" [25], [27]. The trade-off choice adopted between computational cost and results accuracy is further discussed in this work. The validity of the proposed method was evaluated by comparing both attitude and displacement IMU estimations with those obtained through an OPT system.

II. METHODOLOGY AND EXPERIMENTAL SETUP

The strapdown estimation of an IMU displacement from its accelerometer data is a non-trivial task. Let us assume a simplified model of the sensor, where only the linear acceleration is taken into account and the Coriolis, Euler and centripetal accelerations are assumed negligible [28], [29]:

$$\hat{\mathbf{a}}^{\mathcal{B}} = \mathbf{a}_l^{\mathcal{B}} + \mathbf{g}^{\mathcal{B}} + \mathbf{v} \tag{1}$$

where $\mathcal{B}$ represents the sensor's (*Body*) RF. Measured acceleration is a combination of linear acceleration ($\mathbf{a}_l^{\mathcal{B}}$) and gravitational acceleration ($\mathbf{g}^{\mathcal{B}}$) with additive white Gaussian noise denoted as $\mathbf{v} \sim N(0, \mathbf{R})$ [23], [30]. In order to properly estimate the sensor's displacement, three major issues need to be taken into account:

1) The relative orientation estimation of $\mathcal{B}$ with respect to a fixed RF (*Navigation* - $\mathcal{N}$) in which the movement must be represented.
2) The contribution of $\mathbf{g}^{\mathcal{B}}$, which must be efficiently removed before the linear acceleration integration.
3) The integration technique implementation combined with proper filtering to minimize the error introduced by $\mathbf{v}$.

In this section, these points are addressed consequentially. Firstly, an UKF sensor fusion algorithm is proposed to optimally estimate the orientation of the IMU placed on the lower back. Secondly, the estimated orientation is used to properly remove $\mathbf{g}^{\mathcal{B}}$ from each acquired acceleration time frame and refer each accelerometer reading to $\mathcal{N}$. Finally, the double integration of the linear acceleration is performed through a 4th-order Runge-Kutta procedure.

A. Orientation Estimation

The estimation of a rigid body orientation in space amounts to define an algebraic relationship between the representation of a point $\mathbf{p} \in \mathbb{R}^3$ in two different RFs. This relationship is commonly defined using either a Direction Cosine Matrix (DCM) [31] or a quaternion product, as reported in the following expressions:

$$\mathbf{p}^{\mathcal{N}} = \mathbf{A}_{\mathcal{B}}^{\mathcal{N}} \cdot \mathbf{p}^{\mathcal{B}} \tag{2}$$

$$\mathbf{p}^{\mathcal{N}} = [\mathbf{q}_{\mathcal{B}}^{\mathcal{N}}]^{-1} \otimes \mathbf{p}^{\mathcal{B}} \otimes \mathbf{q}_{\mathcal{B}}^{\mathcal{N}} \tag{3}$$

where $\mathbf{p}^{\mathcal{N}}$ and $\mathbf{p}^{\mathcal{B}}$ represent the same point in $\mathbb{R}^3$ respectively in $\mathcal{N}$ and $\mathcal{B}$. For the sake of simplicity, in (2)-(3), $\mathcal{B}$ and $\mathcal{N}$ share the same origin. The matrix $\mathbf{A}_{\mathcal{B}}^{\mathcal{N}}$ is the DCM, whose columns are the axes versors of $\mathcal{B}$ expressed in $\mathcal{N}$. The symbol

$\otimes$ represents the Hamilton Product (HP) [32] and $\mathbf{q}_{\mathcal{B}}^{\mathcal{N}} \in \mathbb{H}$ is a unit quaternion $\mathbf{q} = \begin{bmatrix} q_0 & \mathbf{e}^T \end{bmatrix}^T$, where q_0 is its scalar part and $\mathbf{e}$ is its vector part (or imaginary part) [32].

The quaternion approach offers many advantages over the DCM one. One above all is the possibility to store a 4-D vector instead of a (3×3) matrix. Also, the rotation representation in $\mathbb{H}$ bypasses the gimbal lock issue, which occurs when using Euler angles parametrization. Lastly, this kind of representation allows the feasibility of a state-space approach to orientation estimation, which is presented in the following section.

1) A State-Space Approach: The changing rate of a quaternion describing the orientation of a non-static rigid body, can be related to its angular velocity by the following expression

$$\dot{\mathbf{q}} = \mathbf{\Omega} \cdot \mathbf{q} \tag{4}$$

$$\mathbf{\Omega} = \frac{1}{2} \begin{bmatrix} 0 & -\boldsymbol{\omega}^T \\ \boldsymbol{\omega} & -[\boldsymbol{\omega}\times] \end{bmatrix} \tag{5}$$

where $\boldsymbol{\omega} = \begin{bmatrix} \omega_x & \omega_y & \omega_z \end{bmatrix}^T$ is the rigid body angular velocity expressed in $\mathcal{B}$ and $[\boldsymbol{\omega}\times]$ is a skew-symmetric matrix [33], [34]. The discrete solution of (4) is

$$\mathbf{q}_{k+1} = \mathbf{\Phi}_{k+1,k} \cdot \mathbf{q}_k \tag{6}$$

$$\mathbf{\Phi}_{k+1,k} = \exp(\mathbf{\Omega}_k \cdot T_s) \tag{7}$$

where (7) represents the state-transition matrix of the homogeneous system, which can be approximated to the second term of its Taylor series Expansion as follows:

$$\mathbf{\Phi}_{k+1,k} = \mathbf{I}_{(4\times4)} + \mathbf{\Omega}_k \cdot T_s \tag{8}$$

However, as in the case of the acceleration (1), there is the necessity to deal with real data coming from an estimation of the angular velocity by means of a gyroscope to define the content of (5). Hence

$$\hat{\boldsymbol{\omega}} = \boldsymbol{\omega} + \delta\boldsymbol{\omega} \tag{9}$$

is assumed as a simplified gyroscope model [31], [34], where $\delta\boldsymbol{\omega}$ is a vector Brownian process with $\mathscr{E}\{\delta\boldsymbol{\omega}\delta\boldsymbol{\omega}^T\} = \mathbf{Q}(t)\delta t$ [30] and $\mathscr{E}$ is the expectation operator. The direct consequence of this assumption is the re-definition of (4) as follows:

$$\begin{aligned} \dot{\mathbf{q}} &= (\hat{\mathbf{\Omega}} - \delta\mathbf{\Omega})\mathbf{q} \\ &= \hat{\mathbf{\Omega}}\mathbf{q} - \delta\mathbf{\Omega}\mathbf{q} \\ &= \hat{\mathbf{\Omega}}\mathbf{q} + \mathbf{\Gamma}\delta\boldsymbol{\omega} \end{aligned} \tag{10}$$

with

$$\mathbf{\Gamma} = -\frac{\delta(\mathbf{\Omega}\mathbf{q})}{\delta\boldsymbol{\omega}} = -\frac{1}{2} \begin{bmatrix} -\mathbf{e}^T \\ [\mathbf{e}\times] + q_0 \cdot \mathbf{I} \end{bmatrix} \tag{11}$$

The necessity to involve a filtering process in the orientation estimation is highlighted by the stochastic nature of (10); hence, any attempt to estimate a quaternion from this form would result in unbounded drift after a certain period of time, independently from the numerical integration technique applied.

2) The Filtering Process: A quaternion-based, discrete-time UKF sensor fusion was chosen to estimate the IMU orientation. The state-space vector of the filter is defined by a unit quaternion and the prediction phase of the filter is performed as reported in Table I, where $\mathcal{X}_k$ are the Van Der Merwe Sigma-points at time frame k [35].

The Sigma-points propagation is performed through the $f(*)$ function, which applies the discrete-time model (6)-(7) to the columns of $\mathcal{X}_k$. The system noise covariance matrix is computed as follows, accordingly to [23], [30], [36]:

$$\mathbf{Q}_{k+1} = \left(\frac{T_s}{2}\right)^2 \mathbf{\Gamma}_k \mathbf{\Sigma}_g \mathbf{\Gamma}_k^T \tag{12}$$

where $\mathbf{\Sigma}_g = \sigma_g \mathbf{I}$, and σ_g is the gyroscope sensor's variance. The state error covariance matrix $\mathbf{P}_{k=0}$ and the initial state $\mathbf{q}_{k=0}$ must be obviously given in advance.

The update phase of the filtering process is hence performed by processing the information coming from the accelerometer, as reported in Table II.

The $h(*)$ function (Table II.2) used to propagate the Sigma-points during the update phase is the discrete system's measurement process:

$$\begin{aligned} \hat{\mathbf{a}}_{k+1} &= h(\mathbf{q}_{k+1}^-) + \mathbf{v}_k \\ &= [\mathbf{q}_{k+1}^-]^{-1} \otimes \mathbf{g}_q^{\mathcal{N}} \otimes \mathbf{q}_{k+1}^- + \mathbf{v}_k \end{aligned} \tag{13}$$

with $\mathbf{g}_q^{\mathcal{N}} = \begin{bmatrix} 0 & 0 & 0 & g \end{bmatrix}^T$ quaternion vector [32]. This formulation is made under the assumption that the linear acceleration $\mathbf{a}_l^{\mathcal{B}}$ in the simplified model (1) is small enough to be excluded from the observation at time $(k + 1)$. To achieve this, it is necessary to evaluate the norm of the read acceleration before the update step. In case the norm of the acceleration exceeds g (with a certain tolerance), the assumptions made in (13) fall short, hence the update phase of the filter is skipped and the time index is incremented. The tolerance choice for the acceleration norm evaluation was chosen in compliance with [23].

The high nonlinearity of (13) requires the use of a nonlinear form of the Kalman Filter to estimate the error covariance matrix at the update phase. The UKF is based on the fact that no approximation is made directly on the nonlinear function (model or measurement process), but on its probability distribution [37]. As a result, no first-order approximation is injected in the process through the *a priori* computation of a Jacobian of the nonlinear function (as in EKF). This choice is made in spite of a higher computational complexity due to the Cholesky factorization [38] inside the Unscented transform (UT) step.

B. Displacement Estimation

Thanks to the quaternions estimated in the previous section, it is possible to clean the accelerometer readings from the gravitational component. An estimate of the linear body acceleration is hence given by

$$\mathbf{a}_{l_k}^{\mathcal{N}} \approx \tilde{\mathbf{a}}_{l_k}^{\mathcal{N}} = \mathbf{q}_k \otimes \hat{\mathbf{a}}_k^{\mathcal{B}} \otimes \mathbf{q}_k^{-1} - \mathbf{g}^{\mathcal{N}}; \quad \forall k \tag{14}$$

TABLE I
UKF PREDICTION

Weights computation - *only once*
$c = \alpha^2(\kappa + n); \quad \lambda = c - n$ (I.1)
$w_0^{(m)} = \lambda/c; \quad w_0^{(c)} = \lambda/(c+1-\alpha^2+\beta)$ (I.2)
$w_i^{(m)} = w_i^{(c)} = \lambda/(2c); \quad i = 1 \ldots 2n$ (I.3)
$\mathbf{w}_m = \begin{bmatrix} w_0^{(m)} & w_1^{(m)} & \ldots & w_{2n}^{(m)} \end{bmatrix}^T$ (I.4)
$\mathbf{w}_c = \begin{bmatrix} w_0^{(c)} & w_1^{(c)} & \ldots & w_{2n}^{(c)} \end{bmatrix}^T$ (I.5)
$\mathbf{W} = (\mathbf{I} - \begin{bmatrix} \mathbf{w}_m \ldots \mathbf{w}_m \end{bmatrix}) \cdot \mathrm{diag}(\mathbf{w}_c) \cdot (\mathbf{I} - \begin{bmatrix} \mathbf{w}_m \ldots \mathbf{w}_m \end{bmatrix})^T$ (I.6)

Unscented Transform generation and propagation
$\mathcal{X}_k = \begin{bmatrix} \mathbf{q}_k & \ldots & \mathbf{q}_k \end{bmatrix} + \sqrt{c} \begin{bmatrix} \mathbf{0}_{(n \times 1)} & \sqrt{\mathbf{P}_k^-} & -\sqrt{\mathbf{P}_k^-} \end{bmatrix}$ (I.7)
$\hat{\mathcal{X}}_{k+1} = f(\mathcal{X}_k)$ (I.8)

State and error covariance matrix estimation
$\mathbf{q}_{k+1}^- = \hat{\mathcal{X}}_{k+1}\mathbf{w}_m$ (I.9)
$\mathbf{P}_{k+1}^- = \hat{\mathcal{X}}_{k+1}\mathbf{W}\hat{\mathcal{X}}_{k+1}^T + \mathbf{Q}_{k+1}$ (I.10)

TABLE II
UKF UPDATE

Unscented Transform generation and propagation
$\mathcal{X}_{k+1}^- = \begin{bmatrix} \mathbf{q}_{k+1}^- & \ldots & \mathbf{q}_{k+1}^- \end{bmatrix}$ $+ \sqrt{c} \begin{bmatrix} \mathbf{0}_{(n \times 1)} & \sqrt{\mathbf{P}_{k+1}^-} & -\sqrt{\mathbf{P}_{k+1}^-} \end{bmatrix}$ (II.1)
$\mathcal{Y}_{k+1}^- = h(\mathcal{X}_k^-)$ (II.2)

Kalman Gain computation
$\boldsymbol{\mu}_{k+1} = \mathcal{Y}_{k+1}^- \mathbf{w}_m$ (II.3)
$\mathbf{P}_{k+1}^{xy} = \mathcal{X}_{k+1}^- \mathbf{W}\mathcal{Y}_{k+1}^{-T}$ (II.4)
$\mathbf{P}_{k+1}^{yy} = \mathcal{Y}_{k+1}^- \mathbf{W}\mathcal{Y}_{k+1}^{-T} + \mathbf{R}_k$ (II.5)
$\mathbf{K}_{k+1} = \mathbf{P}_{k+1}^{xy} \mathbf{P}_{k+1}^{yy^{-1}}$ (II.6)

State and error covariance matrix update
$\mathbf{q}_{k+1} = \mathbf{q}_{k+1}^- + \mathbf{K}_{k+1} \cdot (\mathbf{y}_{k+1} - \boldsymbol{\mu}_{k+1})$ (II.7)
$\mathbf{P}_{k+1} = \mathbf{P}_{k+1}^- - \mathbf{K}_{k+1}\mathbf{P}_{k+1}^{yy}\mathbf{K}_{k+1}^T$ (II.8)

where the approximation symbol is due the lack of the noise term $\mathbf{v}$ in the given relationship. The integration of the estimated linear acceleration is carried out via Runge-Kutta 4th-order method [39], solving the following continuous system for $\mathbf{s}$ (speed) and $\mathbf{d}$ (displacement):

$$\dot{\mathbf{s}}_k^{\mathcal{N}} = \tilde{\mathbf{a}}_{l_k}^{\mathcal{N}} \qquad (15)$$

$$\dot{\mathbf{d}}_k^{\mathcal{N}} = \mathbf{s}_k^{\mathcal{N}} \qquad (16)$$

The proposed integration approach relies on the cyclical pattern of acceleration of a sacrum-worn IMU during walking, which allows to compensate drift exploiting the cyclic change of acceleration direction, thus changing the sign of the integration every short temporal interval (left-right stride cycle). The treadmill walking ensures cyclical pattern of acceleration

to be observed on each motion axis (AP, VT and ML). Obtained displacements are further processed with a Butterworth bandpass filter with cutoff frequencies $\omega = [0.1, 5]$ Hz in order to smoothen output signals and deal with residual integration drift.

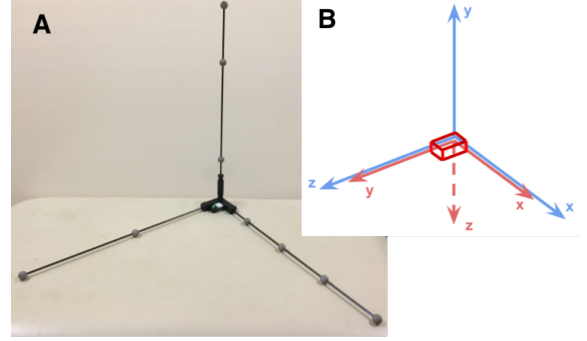### C. Inertial and Navigation Reference Frames Alignment

Fig. 1. As shown in image "A", the inertial sensor is placed to fit the OPT system calibration frame. An example of the relationship between the two different RFs is represented by image "B". In this example, the IMU's RF is rotated of a known 90 deg angle about the OPT system x axis. The $\mathbf{q}_{\text{offset}}$ is hence known.

In order to compare displacements expressed in two different RFs (IMU and OPT system), they must be aligned through a specific calibration procedure. In this regard, due to the lack of magnetometer information for the present setup, the relationship between $\mathcal{B}$ and the chosen $\mathcal{N}$, which is usually obtained considering the heading misalignment with magnetic north. This subsection deals with this fundamental issue to ensure a proper validation of the proposed method through an exact alignment of $\mathcal{B}$ and $\mathcal{N}$.

The filter defined in the previous sections estimates a quaternion which relates the navigation frame $\mathcal{N}$ with $\mathcal{B}$ for every k^{th} instant. Keeping the IMU still and allowing the UKF to converge, for example after i iterations, the resulting estimated quaternion will reflect the rotation which minimizes the residual in (II.7, Table II). The result is hence strictly dependent on the choice of $\mathbf{g}_q^{\mathcal{N}}$. This is however a sub-optimal estimation, since even if the choice of $\mathbf{g}_q^{\mathcal{N}}$ is compliant with the read gravitational component in the wanted $\mathcal{N}$ (in this case the RF of the OPT system), the estimated quaternion is missing an "heading" information, which is usually obtained through a magnetometer. For example, suppose the IMU is laying still on a flat surface with its y-axis pointing upward: choosing $\mathbf{g}_q^{\mathcal{N}} = \begin{bmatrix} 0 & 0 & g & 0 \end{bmatrix}^T$ any quaternion $\mathbf{q}_i = \begin{bmatrix} \cos\theta/2 & 0 & \sin\theta/2 & 0 \end{bmatrix}^T$; $\quad \forall \theta \in \{0, 2\pi\}$ would satisfy (II.7, Table II).

One way to address this issue is to impose the IMU to start the acquisition from a configuration whose orientation ($\mathbf{q}_{\text{offset}}$) with respect to $\mathcal{N}$ is known. The following steps are proposed to ensure a proper alignment:

1) Both the IMU and the target are equipped with small velcro strips.
2) The IMU is placed in the measurement space so that $\mathbf{q}_{\text{offset}}$ is known (Fig. 1). A good choice would be to force

the initial aligment of the two systems chosing $\mathcal{N}$ so that $\mathbf{q}_{\text{offset}} = \begin{bmatrix} 1 & 0 & 0 & 0 \end{bmatrix}^T$.

3) The acquisition starts and the filter is allowed to converge for an arbitrary number of iterations i. This number may change in accordance to how the gyroscope and accelerometer variances affect the $\mathbf{Q}$ and $\mathbf{R}$ matrices and also with the choice of $\mathbf{q}_{k=0}$ and $\mathbf{P}_{k=0}$.

4) The IMU is hence placed on the target thanks to the velcro strips while it is still acquiring.

5) From instant i every quaternion is reset to the $\mathbf{q}_{\text{offset}}$ as follows:

$$\mathbf{q}_k := \mathbf{q}_{\text{offset}} \otimes (\mathbf{q}_i^{-1} \otimes \mathbf{q}_k); \quad \forall k = i \ldots s \qquad (17)$$

where s is the number of samples acquired. This procedure allows the rotations of the IMU to be referred to the RF of the OPT system. As a result, if a ground RF convention is adopted to describe the rotations in terms of roll-pitch-yaw (RPY) angles, any IMU fixed on a markers cluster will return the same estimated values. Consequently, both orientation and displacement estimations can be properly compared between the two measurement systems. Further, the resulting rotations of the rigid body will be always around the axes of the fixed navigation frame, regardless of the different placement of the sensor from one experimental trial to another. This ensures the repeatability and consistency of results among different trials.

D. Experimental Setup and Data Processing

Twelve healthy subjects (6 females and 6 males), age: 23 ± 2, height: 160 ± 10 cm, weight: 60 ± 5 kg were asked to walk on a treadmill for approximately 150 s at a speed of 3, 4 and 5 km/h [40]. Each walking trial was repeated twice for each subject for a total of 72. The total number of steps acquired was 13090 (3335 at 3 km/h, 4602 at 4 km/h and 5153 at 5 km/h). Further, in order to investigate drifting effects, each subject performed three additional longer walking trials (3 km/h) lasting 350 s and the error curve between OPT system and IMU CoM displacement was also computed (see Discussion section). Each subject was instrumented with a single IMU (NGIMU, x-io Technologies (UK), dimensions $56\times39\times18$ mm, weight 46 g, battery life 4-12 hours, sampling rate 100 Hz, triaxial accelerometer: range ±16 g, resolution 490 μg. Triaxial gyroscope: range ±2000 dps, resolution 0.06 $^{\text{deg}}/\text{s}$) attached on a markers cluster placed on the lower trunk (Fig. 2). The cluster hosted a total of four markers and was recorded with a six infrared cameras OPT system (BTS Bioengineering Corp., sampling rate 100 Hz). The markers cluster and IMU placement has been performed for each subject and trial by the same, expert examiner. In order to reduce possible over-controlled conditions in the experimental setup, each subject was instructed to not hold the hands on the handrail, allowing free walking conditions. Accelerometer and gyroscope raw data were off-line processed through a Python custom routine. At the beginning of each trial, the procedure described in Section II-C was followed. This study was conducted following the ethical principles of the Helsinki Declaration and was approved by the local ethics committee.
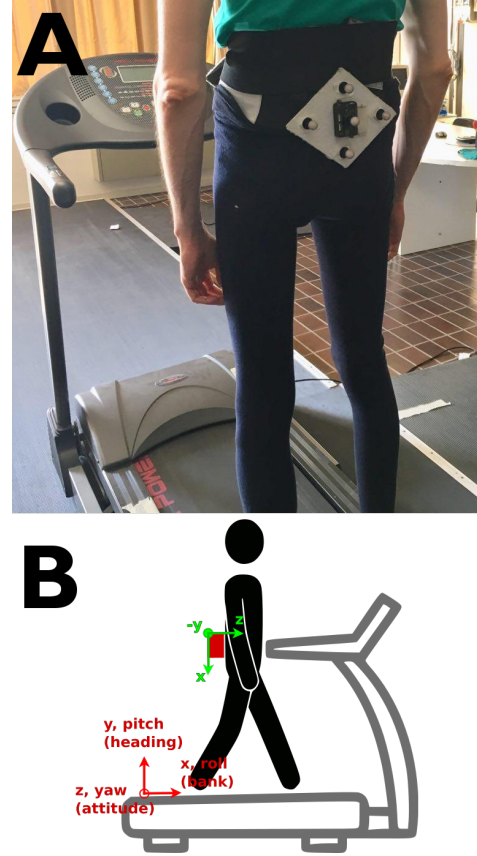

Fig. 2. The IMU was attached in correspondence of the sacrum bone and the rigid markers cluster was fixed with an elastic strap (A). In panel (B) are graphically reported the fixed and navigation RFs.

The volunteers gave their written informed consent prior the beginning of the experiment.

The evaluation of orientation estimation was made comparing the rotations obtained from the two measurement systems. Estimated quaternions for the IMU and rotation matrices from the markers cluster were converted into RPY angles following the $(X_1Y_2Z_3)$ ground Tait-Bryan convention. The angles temporal series were compared in terms of root mean square error (RMSE) and Pearson correlation coefficient (r). The evaluation of IMU displacement was made comparing its peak-to-trough values with the ones extracted from the cameras-measured cluster markers displacement. Further, also the RMSE values between CoM displacement trajectories were computed.

The choice of the RF of the OPT system, in relation to the treadmill, was made as follows: the x axis pointed towards the walking direction, y axis pointed upwards and z axis pointed to form a right-handed coordinate system (Fig. 2).

III. RESULTS

Root mean square errors between RPY angles time-series computed from OPT system and IMU are reported in Table III as mean±standard deviation, together with their correlation coefficients. Peak-to-trough values of the CoM displacement computed from OPT system and IMU data are reported in Table IV, as mean±standard deviation for all the considered

Speed	Rotation axis		RMSE (deg)	SD (deg)	r	p
	Roll	x-axis	1.08	0.93	0.96	10^{-16}
3 km/h	Pitch	y-axis	0.48	0.43	0.96	10^{-16}
	Yaw	z-axis	0.64	0.54	0.92	10^{-16}
	Roll	x-axis	0.95	0.82	0.95	10^{-15}
4 km/h	Pitch	y-axis	0.58	0.51	0.96	10^{-14}
	Yaw	z-axis	0.99	0.92	0.94	10^{-15}
	Roll	x-axis	1.19	0.43	0.97	10^{-16}
5 km/h	Pitch	y-axis	1.43	1.35	0.94	10^{-15}
	Yaw	z-axis	1.79	1.69	0.95	10^{-15}

Speed	Direction		OPT (mm)	IMU (mm)	RMSE (mm)
	AP	x-axis	30.3 ± 11.3	29.3 ± 11.2	1.2 ± 0.5
3 km/h	VT	y-axis	24.6 ± 7.5	25.0 ± 6.5	1.8 ± 1.1
	ML	z-axis	32.7 ± 21.6	32.0 ± 22.2	1.6 ± 0.9
	AP	x-axis	29.2 ± 5.0	30.0 ± 7.0	1.2 ± 0.6
4 km/h	VT	y-axis	30.0 ± 6.0	29.3 ± 9.3	2.1 ± 1.1
	ML	z-axis	45.8 ± 6.9	42.1 ± 8.9	2.4 ± 1.3
	AP	x-axis	26.1 ± 4.5	27.2 ± 6.0	1.4 ± 0.4
5 km/h	VT	y-axis	20.7 ± 5.4	21.8 ± 7.2	2.2 ± 1.3
	ML	z-axis	42.7 ± 6.6	38.4 ± 8.6	2.5 ± 1.3

walking speeds. A boxplot representation of Table IV is given in Fig. 3.

For a representative subject (walking speed 5 km/h), a 20 s window of the RPY angles time series for OPT system and IMU are reported in Fig. 4, while a 20 s time window of CoM displacement computed from OTPS and IMU is reported in Fig. 5.

IV. DISCUSSION

The present work aims to propose a novel software-based technique to estimate the AP, VT, and ML CoM displacement through a sacrum-worn IMU, with respect to a ground RF during treadmill walking along with IMU orientation in a magnetometer-free sensor-fusion setup. Beyond the position estimation drift due to thermal noise integration, which is usually dealt with high-pass filtering, the main issues regarding such practice are the following: the presence of undesired gravitational acceleration readings and the time-varying pose of the sensor's RF. In the present work, a comprehensive approach is proposed to address the listed issues, with an UKF-based filter that estimates the orientation of an IMU with respect to a ground fixed navigation frame. It is worth outlining that the proposed orientation and displacement estimation procedure is performed without using magnetometer data, in contrast with more classical sensor-fusion approaches employing the entire set of information provided by an IMU [23], [28], [41],

[42]. The significant advantage of this approach is its insensitivity to magnetic interferences, which are likely to occur in motion analysis laboratories, where electrical appliances and metallic instrumentation are often present. The latter is well acknowledged as an unavoidable source of distortions which can bias the outcomes of inertial sensing based techniques at various levels [18], [43]. Incidentally, the choice of relying on the above mentioned magnetometer-free sensor fusion, in combination with an UKF-based approach, also allowed to avoid first-order approximation of the measurement model (as in EKF), due to the nature of the UT. An example of first-approximation induced error is shown in Fig. 6, where the drifting behavior of the EKF during a quasi-stationary period is compensated by the UT in the UKF. Despite a direct comparison between EKF and UKF was beyond the aim of the present work and deserves to be deepened in dedicated studies, during the quasi-stationary periods between the end of the calibration procedure and the beginning of walking (about 20 s for each subject), the drifting behavior of the EKF resulted in average initial orientation offsets equal to 13.4±7.7, 1.2±1.0 and 3.3±2.6 degrees for the heading, attitude and bank respectively, while for the UKF the same biases resulted 0.8±0.7, 0.5±0.4 and 0.2±0.1 degrees. It is worth underlining that the latter comparison has been performed under the same filters conditions, i.e. the same initial state and error covariance matrix, same system noise covariance matrix and measurement noise covariance matrix. The above reported differences in the initial biases seem to suggest that the lower performances of EKF in terms of drifting are not directly related to the absence of the magnetic information but it can be referred to the different computational procedures of the two filters, i.e. the measurement model linearization performed by the EKF which is absent in the UKF. However, the probability distribution approximation in the UT, which is achieved through the Cholesky factorization [37], [38], makes the filter barely applicable in real time with an IMU at a working frequency of 100 Hz. At the same time, due to the choice of excluding the magnetometer from the sensor fusion, lower sampling frequencies would make the estimation vulnerable to drift induced by undersampled rapid orientation variations. In this sense, accuracy has been favored over real-time applicability in the present work.

These experimental choices led to the remarkable correspondence of the IMU attitude estimation when compared to that obtained from the gold-standard (OPT system). Indeed, orientation estimation errors (Table III) presented values under 1 deg for both pitch and yaw angles, while the higher errors in the roll angles are due to underestimations of the IMU with respect to the OPT system (Fig. 4). Attitude errors resulted comparable with those reported in [23], when no magnetic disturbances are considered and where a full sensor fusion was performed, i.e. by using also magnetometer data. However, when magnetic disturbances were taken into account, attitude biases reported in [23] raised significantly, resulting higher than those observed for all the walking speeds considered in the present study. These aspects highlight once more the influence of magnetic disturbances on IMU-based attitude estimation. On the other hand, they support the importance
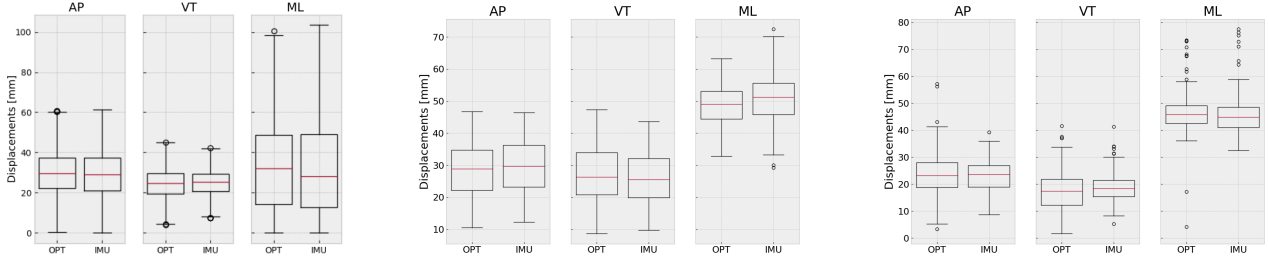
Fig. 3. Boxplot representation of the peak-to-trough estimated from OPT system data and the proposed IMU-based method for 3 km/h (left), 4 km/h (center) and 5 km/h (right). Red lines inside the boxes represent medians. The boxes are defined between the 25th (Q1) and 75th (Q3) percentiles. The whiskers are respectively defined as $Q1 - 1.5 \cdot IQR$ and $Q3 + 1.5 \cdot IQR$, where $IQR = Q3 - Q1$ is the inter-quartile range.
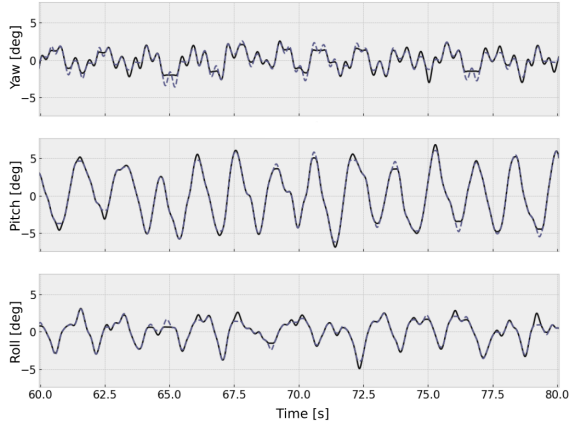

Fig. 4. A 20 s sample window of sacrum-worn IMU rotations of a representative subject estimated through the OPT system (solid line) and the IMU (dashed line) at 5 km/h walking speed. RPY angles (pelvic drop, rotation and anterior tilt respectively as defined by [44]) are respectively referred to rotations about the x, y and z axes of the RF defined in II-D.
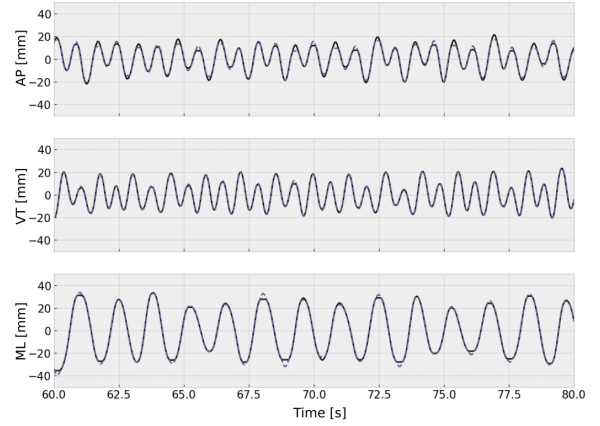
Fig. 5. A 20 s sample window of CoM displacement of a representative subject measured with the OPT system (solid line) and with the IMU (dashed line), at 5 km/h walking speed.

of developing IMU-based orientation estimation methods able to avoid the use of magnetic information, as that proposed in the present study. Incidentally, the reliability of the present results seems to be confirmed also considering full sensor fusion approaches used during the same motor task. Bolink and colleagues [45] proposed an inertial sensor based method for estimating pelvis orientation during gait, reporting errors with respect to an OPT system not lower than 2.6 deg for both sagittal and frontal plane, while in the present study the corresponding angles (yaw and roll) showed a decrease in the RMS errors equal to about 1.5 deg for 3 and 4 km/h and about 1 deg for 5 km/h. The lower and more variable hip angular ranges reported for increased movement speeds [46], could partially account for the higher RMSE and SD observed in IMU orientation, in particular for pitch and yaw angles, when considering increasing walking speeds (Table III). Further, a higher walking speed leads to relatively fast transitions between gait phases, in particular during the loading phase, resulting in faster amplitude transients of inertial data which could likely be linked to an enhanced presence of movement artifact noise in IMU measurements, affecting the eventual

inertial attitude estimation. However, it is worth noticing that the increase in RMSE and SD values for 4 and 5 km/h is in any case not higher than 1 deg with respect to 3 km/h, highlighting a reliable attitude estimation also for increasing walking speeds.

An accurate orientation estimation of an IMU is crucial for its 3-D displacement computation, considering that a good orientation estimation positively affects an efficient removal of the gravitational component. However, a correct rotation of the read acceleration to fit the navigation frame is unavoidable when displacement estimation has to be represented in an arbitrary coordinate system, other than the sensor RF; this is also true when those estimations have to be compared to the measurements provided by a gold-standard OPT system for validation purposes. Therefore, in order to address the latter issues, a straightforward calibration procedure is proposed (Section II-C) to refer magnetometer-free orientation estimation to a fixed RF.

With regard to this matter, it is important to note that, without the proposed calibration, the lack of magnetic information in the present experimental setup would make it

impossible to refer the body RF of the IMU to a ground-fixed RF, which is usually determined by a standard heading rotation with respect to the measured magnetic north. Henceforth, any estimated displacement would not be related to the real VT, ML, and AP directions. Despite it is often disregarded, this aspect is of paramount importance in order to obtain a proper measurement reference to a fixed RF. Indeed, without this kind of calibration, the following orientation and displacement estimation of the sensor would be referenced to the initial pose of the sensor, which depends on the *in situ* placement procedure made by the experimenter. Keeping in mind the proposed application, the misalignment of the sensor RF with respect to a fixed RF is to be considered as an unavoidable issue, due to three main leading factors: the first is the physiological shape of the human pelvis and in general of the human back, which is not normal to the ground plane. The second is the intra- and inter-examiner variability in the sensor placement and the third is the difficulty to obtain a perfect alignment of the subject, and thus of the sensor heading, with the direction of progression. All of these factors lead to a misalignment between the sensor's and the fixed RFs which, if not properly addressed, represents a significant source of error when the orientation and displacement estimated from the IMU are compared with those measured in the fixed RF.

In the present study, thanks to the calibration procedure, it was possible to estimate and correct, for each trial, the starting sensor misalignments with respect to the fixed RF. Average sensor misalignments showed non negligible values, equal to 3.0±4.0 deg for the roll angle, 0.5±2.2 deg for the pitch angle and 6.5±5.7 deg for the yaw angle. Therefore, the proposed calibration procedure was needed in order to make the measurement setup immune to the above mentioned subject heading misalignment (mainly affecting pitch estimation and leading to AP and ML displacement estimation errors), lower-back cluster placement errors (mainly affecting yaw estimation and leading to VT and AP displacement estimation errors) and IMU positioning on the cluster (mainly affecting roll estimation and leading to VT and ML displacement estimation errors).

Results in displacement estimations have been evaluated comparing the peak-to-trough distances computed from the OPT system and IMU time-series. The high similarities between percentiles of the two sets of measures show that the two systems are measuring the same quantities (25%, 50% and 75% percentile absolute differences are below 2 mm for each axis and for each walking speed, Fig. 3). Further, at 3 km/h both the average peak-to-trough and standard deviations numerical values measured by the two systems resulted in any case below 1 mm (Table IV) for each considered direction. For the other two considered speeds, only the ML direction showed a limited increase in the errors, not higher than 4 mm, with similar standard deviations. This indicates that the measurements performed by the proposed IMU-based method and the OPT system agree not only in terms of average values but also in terms of inter-subject variability.

In particular, regarding the vertical CoM component, present results showed errors 80% lower with respect to [47] where the same experimental setup was adopted, but higher speeds were
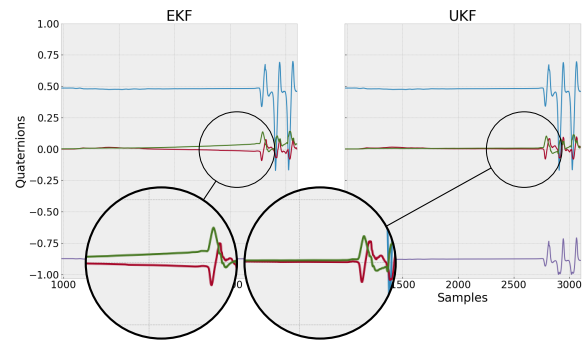

Fig. 6. Example of quaternions estimated with EKF and UKF. The EKF shows a significant drifting behavior toward the end of the stationary period, which is absent in the UKF estimation. Circles represent a magnified view of the different drifting behavior of EKF and UKF.
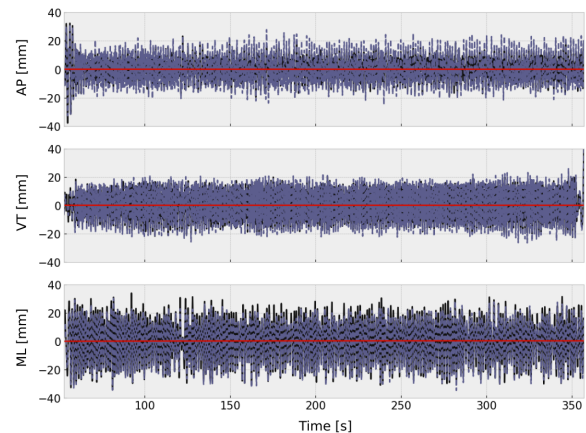

Fig. 7. CoM displacement time-series along the AP, VT and ML directions during a 350 s walking trial of a representative subject. Red line represents the error between OPT system (solid line) and IMU (dashed line).

considered. Considering other works where a full sensor fusion (including magnetometer) was performed, our estimation accuracy of VT CoM component resulted comparable for all the gait speeds with that reported in [13], where a lower number of consecutive free walking cycles was considered (three walks). The accuracy was also higher with respect to [48] (about 2 mm versus an average error over the three speeds of about 0.6 mm), where a 10 m walking test was performed and two consecutive steps were analyzed and with respect to [49], where 10 s walking trials were analyzed. Incidentally, the accuracy on the VT CoM component results particularly important, being a valuable source of information about gait mechanics and one of the most considered features for the latter kind of motor task [4]. Despite relatively few studies compared the full 3-D CoM trajectory estimation during walking obtained by a single IMU, for what concerns the AP and VT CoM components, the errors obtained in the present study resulted not higher than 1 mm for all the considered walking speeds (Table IV), while in [11] errors not lower than 3 mm were reported for the same

directions, with a remarkable drop of the error of about 80% (about 0.5 mm versus 3 mm) for the VT direction. For the ML component, the errors resulted comparable for trials at 4 and 5 km/h, while for trials at 3 km/h they showed a considerably lower value (about 0.4 mm versus 3 mm). Incidentally, the accuracy of displacement estimation seems to be supported also by the RMSE values between CoM trajectories (Table IV), which resulted in any case below 2.5 mm for 150 s walking trials, with a limited variability (SD not higher than 1.3 mm). It is worth noticing that in [11] only the subjects' self-selected speed was considered and more importantly there was the need for a multi-IMU setup for CoM estimation, while in the present study a noticeably less obtrusive setup was presented, with a single sacrum-worn sensor.

Eventually, another aspect deserves to be briefly discussed. When dealing with strapdown inertial motion tracking, the drifting issue represents an aspect to be carefully dealt with. The solutions reported in Section II-B appear to properly address the drift issue for relatively long walking trials (150 s) at 3, 4 and 5 km/h. However, the reliability of the proposed approach has been verified also considering longer epochs. Therefore, each subject performed three additional walking trials lasting 350 s and the convergence in measure [50] was studied through the computation of the error curve. As shown in Fig. 7, the absence of any significant drifting effect is verified by the quasi-static value of the average error convergence to zero.

The proposed CoM estimation method provides promising results in terms of both orientation and 3-D displacement, also when the walking task was performed at different speeds (3, 4 and 5 km/h). However, it is worth noticing that, taking into account the experimental setup employed in this study, a direct comparison with one of the most used methods for CoM estimation, i.e. the segmental analysis, was not performed. Albeit it was beyond the aim of the study, the latter could be viewed as a partial limitation of this work, deserving to be carefully investigated in future and focused studies. However, the validity of the present results with respect to a widely used and accepted CoM estimation method, i.e. the sacral marker method, seems to suggest the reliability of the proposed procedure also with respect to different CoM estimation methods. Indeed, for the walking task the sacral marker method has been reported to be comparable with respect to the segmental analysis [9], [10] and even better with respect to different methods, such as those based on the double integration of the ground reaction force [9]. However, all these aspects need to be deepened and investigated in dedicated studies, also considering larger populations and different gait conditions, such as ground and slope walking.

Future studies should assess the validity of the proposed CoM estimation procedure with respect to the segmental analysis method, by using a multi-IMU setup. Further, the 3-D CoM displacement based on a single IMU should be tested also on level walking, where a different strapdown procedure is needed for an IMU placed on the sacrum and not on the foot [19]. The use of the magnetometer information also deserves to be carefully assessed, in order to better understand the weight of such kind of data in this type of applications. Eventually, due the off-line processing presented in this study for 3-D orientation and displacement estimation, the real-time applicability of the proposed procedure deserves to be carefully investigated. The latter, together with a stand-alone version of the proposed algorithm, represents a part of the future developments regarding this work. Incidentally, a generalized version of the proposed algorithm is currently under development and will be made available upon request on a public hosting service (GitLab) for those interested.

V. Conclusion

In this work, a single IMU and RF alignment procedure to estimate 3-D CoM displacement and orientation during treadmill walking has been presented. Magnetometer-free sensor fusion has been proposed to avoid orientation estimation errors introduced by the treadmill structure and electric motor, and more generally to be applied in any laboratory environment where magnetic disturbances may affect measurements.

The proposed approach relies on a *Unscented* variant of the Kalman Filter and on post-processing Butterworth filters, highlighting a focus on data accuracy with low-cost instrumentation rather than real-time applicability, which is most valuable in clinical settings. The compact form of the proposed algorithm, alongside with a straightforward ground-fixed RF alignment procedure, the necessity of a single low-cost measuring device such as an IMU and the use of a common electrical treadmill, make this experimental setup highly valuable in those scenarios where cumbersome instrumentation is willingly avoided to ensure subject's freedom of movement.

References

[1] E. M. Gutierrez-Farewik, A. Bartonek, and H. Saraste, "Comparison and evaluation of two common methods to measure center of mass displacement in three dimensions during gait," *Human Movement Science*, vol. 25, no. 2, pp. 238–256, 2006.

[2] J. Collett, H. Dawes, K. Howells, C. Elsworth, H. Izadi, and C. Sackley, "Anomalous centre of mass energy fluctuations during treadmill walking in healthy individuals," *Gait & Posture*, vol. 26, no. 3, pp. 400–406, 2007.

[3] A. H. Huntley, A. Schinkel-Ivy, A. Aqui, and A. Mansfield, "Validation of simplified centre of mass models during gait in individuals with chronic stroke," *Clinical Biomechanics*, vol. 48, pp. 97–102, 2017.

[4] L. Tesio and V. Rota, "The motion of body center of mass during walking: a review oriented to clinical applications," *Frontiers in Neurology*, vol. 10, p. 999, 2019.

[5] H.-J. Lee and L.-S. Chou, "Detection of gait instability using the center of mass and center of pressure inclination angles," *Archives of Physical Medicine and Rehabilitation*, vol. 87, no. 4, pp. 569–575, 2006.

[6] J. Feng, R. Pierce, K. P. Do, and M. Aiona, "Motion of the center of mass in children with spastic hemiplegia: balance, energy transfer, and work performed by the affected leg vs. the unaffected leg," *Gait & Posture*, vol. 39, no. 1, pp. 570–576, 2014.

[7] A. Opheim, J. McGinley, E. Olsson, J. Stanghelle, and R. Jahnsen, "Walking deterioration and gait analysis in adults with spastic bilateral cerebral palsy," *Gait & Posture*, vol. 37, no. 2, pp. 165–171, 2013.

[8] J. Eng and D. Winter, "Estimations of the horizontal displacement of the total body centre of mass: considerations during standing activities," *Gait & Posture*, vol. 1, no. 3, pp. 141–144, 1993.

[9] M. Saini, D. Kerrigan, M. Thirunarayan, and M. Duff-Raffaele, "The vertical displacement of the center of mass during walking: a comparison of four measurement methods," *Journal of Biomechanical Engineering*, vol. 120, no. 1, pp. 133–139, 1998.

[10] B. Jeong, C.-Y. Ko, Y. Chang, J. Ryu, and G. Kim, "Comparison of segmental analysis and sacral marker methods for determining the center of mass during level and slope walking," *Gait & Posture*, vol. 62, pp. 333–341, 2018.

[11] M. J. Floor-Westerdijk, H. M. Schepers, P. H. Veltink, E. H. van Asseldonk, and J. H. Buurke, "Use of inertial sensors for ambulatory assessment of center-of-mass displacements during walking," *IEEE Transactions on Biomedical Engineering*, vol. 59, no. 7, pp. 2080–2084, 2012.

[12] F. Yang and Y.-C. Pai, "Can sacral marker approximate center of mass during gait and slip-fall recovery among community-dwelling older adults?" *Journal of Biomechanics*, vol. 47, no. 16, pp. 3807–3812, 2014.

[13] P. Esser, H. Dawes, J. Collett, and K. Howells, "Imu: inertial sensing of vertical com movement," *Journal of Biomechanics*, vol. 42, no. 10, pp. 1578–1581, 2009.

[14] F. Buganè, M. G. Benedetti, V. D'Angeli, and A. Leardini, "Estimation of pelvis kinematics in level walking based on a single inertial sensor positioned close to the sacrum: validation on healthy subjects with stereophotogrammetric system," *Biomedical Engineering Online*, vol. 13, no. 1, p. 146, 2014.

[15] R. S. McGinnis, S. M. Cain, S. Tao, D. Whiteside, G. C. Goulet, E. C. Gardner, A. Bedi, and N. C. Perkins, "Accuracy of femur angles estimated by imus during clinical procedures used to diagnose femoroacetabular impingement," *IEEE Transactions on Biomedical Engineering*, vol. 62, no. 6, pp. 1503–1513, 2015.

[16] S. Hesse, B. Helm, J. Krajnik, M. Gregoric, and K. H. Mauritz, "Treadmill training with partial body weight support: influence of body weight release on the gait of hemiparetic patients," *Journal of Neurologic Rehabilitation*, vol. 11, no. 1, pp. 15–20, 1997.

[17] N. A. Segal, N. A. Glass, P. Teran-Yengle, B. Singh, R. B. Wallace, and H. J. Yack, "Intensive gait training for older adults with symptomatic knee osteoarthritis," *American Journal of Physical Medicine & Rehabilitation/Association of Academic Physiatrists*, vol. 94, no. 10 0 1, p. 848, 2015.

[18] W. De Vries, H. Veeger, C. Baten, and F. Van Der Helm, "Magnetic distortion in motion labs, implications for validating inertial magnetic sensors," *Gait & Posture*, vol. 29, no. 4, pp. 535–541, 2009.

[19] E. Foxlin, "Pedestrian tracking with shoe-mounted inertial sensors," *IEEE Computer Graphics and Applications*, no. 6, pp. 38–46, 2005.

[20] H. Weinberg, "Using the adxl202 in pedometer and personal navigation applications," *Analog Devices AN-602 Application Note*, vol. 2, no. 2, pp. 1–6, 2002.

[21] L. Pepa, F. Verdini, and L. Spalazzi, "Gait parameter and event estimation using smartphones," *Gait & Posture*, vol. 57, pp. 217–223, 2017.

[22] X. Yun, E. R. Bachmann, H. Moore, and J. Calusdian, "Self-contained position tracking of human movement using small inertial/magnetic sensor modules," in *Robotics and Automation, 2007 IEEE International Conference on*. IEEE, 2007, pp. 2526–2533.

[23] A. M. Sabatini, "Quaternion-based extended kalman filter for determining orientation by inertial and magnetic sensing," *IEEE Transactions on Biomedical Engineering*, vol. 53, no. 7, pp. 1346–1356, 2006.

[24] S. Sabatelli, M. Galgani, L. Fanucci, and A. Rocchi, "A double-stage kalman filter for orientation tracking with an integrated processor in 9-d imu," *IEEE Transactions on Instrumentation and Measurement*, vol. 62, no. 3, pp. 590–598, 2012.

[25] E. A. Wan and R. Van Der Merwe, "The unscented kalman filter for nonlinear estimation," in *Adaptive Systems for Signal Processing, Communications, and Control Symposium 2000. AS-SPCC. The IEEE 2000*. Ieee, 2000, pp. 153–158.

[26] N. Enayati, E. De Momi, and G. Ferrigno, "A quaternion-based unscented kalman filter for robust optical/inertial motion tracking in computer-assisted surgery," *IEEE Transactions on Instrumentation and Measurement*, vol. 64, no. 8, pp. 2291–2301, 2015.

[27] G. Terejanu, T. Singh, and P. D. Scott, "Unscented kalman filter/smoother for a cbrn puff-based dispersion model," in *Information Fusion, 2007 10th International Conference on*. IEEE, 2007, pp. 1–8.

[28] G. Ligorio and A. M. Sabatini, "A novel kalman filter for human motion tracking with an inertial-based dynamic inclinometer." *IEEE Transactions on Biomedical Engineering*, vol. 62, no. 8, pp. 2033–2043, 2015.

[29] J. K. Lee, E. J. Park, and S. N. Robinovitch, "Estimation of attitude and external acceleration using inertial sensor measurement during various dynamic conditions," *IEEE Transactions on Instrumentation and Measurement*, vol. 61, no. 8, pp. 2262–2273, 2012.

[30] A. H. Jazwinski, *Stochastic Processes and Filtering Theory*. Courier Corporation, 2007.

[31] M. D. Shuster and S. D. Oh, "Three-axis attitude determination from vector observations," *Journal of Guidance, Control, and Dynamics*, vol. 4, no. 1, pp. 70–77, 1981.

[32] E. Abbena, S. Salamon, and A. Gray, *Modern Differential Geometry of Curves and Surfaces with Mathematica*. Chapman and Hall/CRC, 2017.

[33] J. E. Bortz, "A new mathematical formulation for strapdown inertial navigation," *IEEE Transactions on Aerospace and Electronic Systems*, no. 1, pp. 61–66, 1971.

[34] I. Bar-Itzhack and Y. Oshman, "Attitude determination from vector observations: Quaternion estimation," *IEEE Transactions on Aerospace and Electronic Systems*, no. 1, pp. 128–136, 1985.

[35] R. Van Der Merwe *et al.*, "Sigma-point kalman filters for probabilistic inference in dynamic state-space models," Ph.D. dissertation, OGI School of Science & Engineering at OHSU, 2004.

[36] D. Choukroun, I. Y. Bar-Itzhack, and Y. Oshman, "Novel quaternion kalman filter," *IEEE Transactions on Aerospace and Electronic Systems*, vol. 42, no. 1, pp. 174–190, 2006.

[37] S. J. Julier and J. K. Uhlmann, "New extension of the kalman filter to nonlinear systems," in *Signal Processing, Sensor Fusion, and Target Recognition VI*, vol. 3068. International Society for Optics and Photonics, 1997, pp. 182–193.

[38] S. Sarkka, "On unscented kalman filtering for state estimation of continuous-time nonlinear systems," *IEEE Transactions on Automatic Control*, vol. 52, no. 9, pp. 1631–1641, 2007.

[39] J. R. Dormand and P. J. Prince, "A family of embedded runge-kutta formulae," *Journal of Computational and Applied Mathematics*, vol. 6, no. 1, pp. 19–26, 1980.

[40] R. Dickstein and Y. Laufer, "Light touch and center of mass stability during treadmill locomotion," *Gait & Posture*, vol. 20, no. 1, pp. 41–47, 2004.

[41] M. Jin, J. Zhao, J. Jin, G. Yu, and W. Li, "The adaptive kalman filter based on fuzzy logic for inertial motion capture system," *Measurement*, vol. 49, pp. 196–204, 2014.

[42] G. E. Kang and M. M. Gross, "Concurrent validation of magnetic and inertial measurement units in estimating upper body posture during gait," *Measurement*, vol. 82, pp. 240–245, 2016.

[43] R. D. Gurchiek, R. S. McGinnis, A. R. Needle, J. M. McBride, and H. van Werkhoven, "The use of a single inertial sensor to estimate 3-dimensional ground reaction force during accelerative running tasks," *Journal of Biomechanics*, vol. 61, pp. 263–268, 2017.

[44] J. Perry, J. R. Davids *et al.*, "Gait analysis: normal and pathological function." *Journal of Pediatric Orthopaedics*, vol. 12, no. 6, p. 815, 1992.

[45] S. Bolink, H. Naisas, R. Senden, H. Essers, I. Heyligers, K. Meijer, and B. Grimm, "Validity of an inertial measurement unit to assess pelvic orientation angles during gait, sit–stand transfers and step-up transfers: Comparison with an optoelectronic motion capture system," *Medical Engineering & Physics*, vol. 38, no. 3, pp. 225–231, 2016.

[46] H. J. Bennett, K. Fleenor, and J. T. Weinhandl, "A normative database of hip and knee joint biomechanics during dynamic tasks using anatomical regression prediction methods," *Journal of Biomechanics*, vol. 81, pp. 122–131, 2018.

[47] R. Watari, B. Hettinga, S. Osis, and R. Ferber, "Validation of a torso-mounted accelerometer for measures of vertical oscillation and ground contact time during treadmill running," *Journal of Applied Biomechanics*, vol. 32, no. 3, pp. 306–310, 2016.

[48] P. Esser, H. Dawes, J. Collett, M. G. Feltham, and K. Howells, "Validity and inter-rater reliability of inertial gait measurements in parkinson's disease: a pilot study," *Journal of Neuroscience Methods*, vol. 205, no. 1, pp. 177–181, 2012.

[49] D. Steins, I. Sheret, H. Dawes, P. Esser, and J. Collett, "A smart device inertial-sensing method for gait analysis," *Journal of Biomechanics*, vol. 47, no. 15, pp. 3780–3785, 2014.

[50] A. Papoulis and H. Saunders, *Probability, random variables and stochastic processes*. American Society of Mechanical Engineers Digital Collection, 1989.

Stefano Cardarelli received his MS degree (summa cum laude) in Electronic Engineering at Università Politecnica delle Marche in 2016. He is currently working toward the Ph.D. degree in Information Engineering at the same institute. His main research topic involves postural and dynamical studies in human locomotion via inertial measurement units and advanced filtering and optimization techniques. He has also collaborated on projects regarding electromyography signal processing and application of control theory to the analysis of balance during dynamical perturbations.

Francesco Di Nardo is currently Staff Scientist at the Movement Analysis and Bioengineering Lab (LAMB), Department of Information Engineering, Università Politecnica delle Marche, Ancona, Italy. He received his Ph.D. in Artificial Intelligence Systems, in 2005 at Università Politecnica delle Marche, Italy. His main research activity includes the field of movement analysis for motor rehabilitation, with particular involvement in acquisition and processing of surface electromyography signal to assess the muscular function during gait task. He is also involved in the development and the clinical application (type-2 diabetes, insulin resistance and hypertension) of mathematical models of metabolic and endocrine systems in humans and in their animal models. He participated in various National research projects. He published several papers in peer review international journals, books and conference proceedings.

Alessandro Mengarelli received the MS degree in Biomedical Engineering and the Ph.D. degree in Information Engineering from Università Politecnica delle Marche, Ancona, Italy, in 2012 and 2017, respectively. Currently, his research interests involve biomechanics of movement in both static and dynamic conditions, the application of control theory and modeling to the analysis of balance in perturbed conditions, with a multibody dynamic approach and the non-linear analysis of static balance. Further, he is also involved in the assessment of muscular functions during gait through the electromyography signal processing. In these fields, he authored/coauthored scientific publications in peer reviewed international journals and conference proceedings.

Sandro Fioretti graduated in 1979 in Electronic Engineering at Ancona University and presently is Associate Professor in Bioengineering at the Department of Information Engineering – Università Politecnica delle Marche - Ancona. He teaches Movement Biomechanics and Bioengineering of Motor Rehabilitation at the Biomedical Engineering course of the same University. His main research interests are in the field of human movement analysis and its related fields such as: stereophotogrammetry, linear and nonlinear filtering, joint kinematics, analysis and identification of postural control, static and perturbed posturography, gait analysis, dynamic electromyography. He participated in various European and National research projects in the field of movement analysis for motor rehabilitation. He is author of numerous scientific publications in international journals, books and congress proceedings.

Andrea Tigrini received the MS degree in Biomedical Engineering from Università Politecnica delle Marche, Ancona, Italy, in 2018. Currently, he is a Ph.D. student in Information Engineering at Università Politecnica delle Marche. His research interests involve the study of human biomechanics, neuromuscular control and rehabilitation engineering. In these fields, he authored/coauthored scientific publications in international journals and conference proceedings.

Federica Verdini obtained her MS degree in Electronic Engineering at the Ancona University in 1997 and the Ph.D degree in Bioengineering at the Bologna University in 2001. Her research activity focuses on the recording and processing of biological signals associated with human movement and on the study of control models related to motion and posture. In these fields she authored many scientific publications in international journals, books and conference proceedings. Currently she is Chief-staff scientist at the Movement analysis and Bioengineering Laboratory (LAMB) of the Università Politecnica delle Marche and teaches the class of Automatic Control for the course of Biomedical and Electronic engineering at Università Politecnica delle Marche. She has been involved in many European and national research projects.

Annachiara Strazza received the MS degree in Electronic Engineering and the Ph.D. degree in Information Engineering from Università Politecnica delle Marche, Ancona, Italy, in 2015 and 2019, respectively. Her main research interests include gait analysis to assess the muscles' behavior and the surface electromyographic signal (sEMG) processing in time-frequency domain in dynamic tasks for clinical purpose. In this field, she is author of scientific publications in international journals and conference proceedings.